MEDICAL SCIENCE MONITOR

ANIMAL STUDY

e-ISSN 1643-3750
© Med Sci Monit, 2018; 24: 511-522
DOI: 10.12659/MSM.905442

Received: 2017.05.23
Accepted: 2017.07.13
Published: 2018.01.26

The Role of miR-126 in Critical Limb Ischemia Treatment Using Adipose-Derived Stem Cell Therapeutic Factor Concentrate and Extracellular Matrix Microparticles

Authors' Contribution:
Study Design A
Data Collection B
Statistical Analysis C
Data Interpretation D
Manuscript Preparation E
Literature Search F
Funds Collection G

ABCDEFG 1 Václav Procházka
ABDEFG 2 Jana Jurčíková
ABDEFG 2 Kateřina Vítková
CD 2 Lubomír Pavliska
ABDEFG 3 Ludmila Porubová
CD 3 Ondrej Lassák
BDEF 4 Piotr Buszman
ABDE 4 Carlos A. Fernandez
AB 5 František Jalůvka
BDE 6 Iveta Špačková
BDE 7 Ivo Lochman
ADEF 8 Martin Procházka
ADEF 8,9 Mária Janíková
ADEF 10 Zdeněk Tauber
ADEF 11 Jana Franková
BDE 2 Martin Lachnit
DE 12 Michael C. Hiles
ADEF 13 Brian H. Johnstone

1 Radiodiagnostic Institute, University Hospital Ostrava, Ostrava, Czech Republic
2 Department of Deputy Director of Science and Research, University Hospital Ostrava, Ostrava, Czech Republic
3 4MEDi-CBTD, Ostrava, Czech Republic
4 American Heart of Poland, Inc., Katowice, Poland
5 Department of Surgery, University Hospital Ostrava, Ostrava, Czech Republic
6 Laboratoře AGEL, a.s., Nový Jičín, Czech Republic
7 SPADIA LAB a.s., Ostrava, Czech Republic
8 Department of Medical Genetics, University Hospital Olomouc and Palacky University Olomouc, Olomouc, Czech Republic
9 Department of Clinical and Molecular Pathology, Palacky University Olomouc and University Hospital Olomouc, Olomouc, Czech Republic
10 Department of Histology and Embryology, Faculty of Medicine and Dentistry, Palacky University Olomouc, Olomouc, Czech Republic
11 Department of Medical Chemistry and Biochemistry, Faculty of Medicine and Dentistry, Palacky University Olomouc, Olomouc, Czech Republic
12 Cook Biotech, Inc., West Lafayette, IN, U.S.A.
13 NeuroFX, LLC, Indianapolis, IN, U.S.A.

Corresponding Author: Václav Procházka, e-mail: vaclav.prochazka@fno.cz
Source of support: This work was supported by the Ministry of Education, Youth, and Sports, Czech Republic, GESHER/MOST Program, project no. LJ14003 (DiaCellix – new regenerative medicine product for the treatment of secondary effects of T2DM) and by RVO: 61989592.

Background: Paracrine factors secreted by adipose-derived stem cells can be captured, fractionated, and concentrated to produce therapeutic factor concentrate (TFC). The present study examined whether TFC effects could be enhanced by combining TFC with a biological matrix to provide sustained release of factors in the target region.

Material/Methods: Unilateral hind limb ischemia was induced in rabbits. Ischemic limbs were injected with either placebo control, TFC, micronized small intestinal submucosa tissue (SIS), or TFC absorbed to SIS. Blood flow in both limbs was assessed with laser Doppler perfusion imaging. Tissues harvested at Day 48 were assessed immunohistochemically for vessel density; *in situ* hybridization and quantitative real-time PCR were employed to determine miR-126 expression.

Results: LDP ratios were significantly elevated, compared to placebo control, on day 28 in all treatment groups (p=0.0816, p=0.0543, p=0.0639, for groups 2-4, respectively) and on day 36 in the TFC group (p=0.0866). This effect correlated with capillary density in the SIS and TFC+SIS groups (p=0.0093 and p=0.0054, respectively, compared to placebo). A correlation was observed between miR-126 levels and LDP levels at 48 days in SIS and TFC+SIS groups.

Conclusions: A single bolus administration of TFC and SIS had early, transient effects on reperfusion and promotion of ischemia repair. The effects were not additive. We also discovered that TFC modulated miR-126 levels that were expressed in cell types other than endothelial cells. These data suggested that TFC, alone or in combination with SIS, may be a potent therapy for patients with CLI that are at risk of amputation.

MeSH Keywords: Culture Media, Conditioned • *In Situ* Hybridization • MicroRNAs • Stem Cell Research

Full-text PDF: https://www.medscimonit.com/abstract/index/idArt/905442

4643 2 7 47

Indexed in: [Current Contents/Clinical Medicine] [SCI Expanded] [ISI Alerting System] [ISI Journals Master List] [Index Medicus/MEDLINE] [EMBASE/Excerpta Medica] [Chemical Abstracts/CAS]

Background

The non-adipocyte stromal vascular fraction (SVF) of human adipose tissues contains a population of mesenchymal stem cells (MSCs) intimately associated with blood vessels [1]. These adipose tissue-derived stem cells (ASCs) possess many phenotypic and functional similarities to bone marrow-derived MSCs (BM-MSCs). However, unlike BM-MSCs, multipotent ASCs can be harvested at relatively high numbers (0.5×10^6/g fat, in a typical harvest of 500 g tissue) with minimally invasive techniques (i.e., lipoaspiration or lipectomy) from subcutaneous adipose tissue [2]. ASCs rapidly proliferate in culture. This rapid expansion achieves cell quantities sufficient for treating large-volume lesions. Transplantation of ASCs is an emerging therapeutic option for addressing many intractable diseases, including cardiovascular diseases, such as peripheral artery disease (PAD) [3–8].

Currently, evidence suggests that the therapeutic effects of MSCs, including ASCs, are primarily mediated through paracrine mechanisms, rather than cellular transdifferentiation [9–12]. We recently demonstrated this effect directly by administering a concentrated secretome harvested from ASCs to the affected limb in a rabbit model of subacute critical limb ischemia (CLI) [13]. That study demonstrated robust repair of the ischemic limb with a cell-free ASC-derived therapeutic factor concentrate (TFC). The degree of reperfusion in ischemic limbs was dose-dependent, and it correlated with increased capillary density. Although the effect of a low dose was not significant, we observed an early trend of increased perfusion in this group of animals, which abated by the end of the study. That finding suggested the possibility that the effects were transitory, and might be enhanced by prolonging exposure to TFC by either repeating the treatment or by encapsulating or binding the TFC to matrices to provide sustained release.

It is well known that the extracellular matrix (ECM) serves as a repository of cytokines that modulate cellular behavior [14]. The 2 components of natural ECMs most responsible for factor binding are heparin and heparan sulfate proteoglycan, and both are glycosaminoglycans (GAGs). Furthermore, these GAGs bind to the charged regions found in most growth factors, including the potent angiogenic proteins, basic fibroblast growth factor (bFGF) and vascular endothelial growth factor (VEGF) (recently reviewed) [15]. Many of the factors identified in TFC, including monocyte chemoattractant protein (CCL2), hepatocyte growth factor (HGF), and insulin-like growth factor 1 (IGF-1), are heparin-binding molecules. Indeed, some of these factors, such as CCL2 and epithelial neutrophil-activating peptide 78 (CXCL5), must be bound to GAGs for functional activity [16,17].

In the present study, we tested a method for delivering TFC complexed to SIS, where SIS was in a micronized form, suitable for injection. These particles had an average diameter of 120 µm, and they were largely composed of collagen, GAGs, and fibronectin; moreover, they contained some inherent growth factors [18]. Thus, in addition to binding to TFC, the GAGs, particularly heparan sulfates, are important regulators of biological process, including angiogenesis, which are required for repairing ischemic tissues [15,19]. SIS has been used effectively, as a stand-alone therapy, in numerous clinical applications, including cutaneous and surgical wound healing applications [20,21]. Therefore, for the present study, SIS was a logical choice for use as a carrier, because it might provide sustained release of TFC factors and promote their retention, when injected in the region of injury [22–26]. We employed the subacute rabbit CLI model to examine whether TFC complexed with SIS could enhance the beneficial effects observed in an earlier study that tested a single administration of TFC alone (also in the rabbit CLI model). Additionally, we conducted a long-term follow-up to determine whether the effects persisted.

This study also aimed to determine the mechanisms by which a single TFC administration could stimulate a sustained pro-angiogenic response in the host, as reported earlier. We hypothesized that a regulatory RNA, specifically a microRNA (miRNA), might contribute to the effects. miRNAs are small non-coding RNA molecules (~22 nucleotides) that control expression of thousands of human genes at the post-transcriptional level, by binding to target mRNAs and interfering with transcription. The binding of miRNAs is based on homology to target sequences, mainly localized in the 3´ untranslated regions (3' UTRs) of mRNA molecules [27,28]. Many miRNAs are involved in regulating biological processes, including cell growth and proliferation [29]. In particular, miR-126 is highly enriched in endothelial cells and platelets. Previously, miR-126 was shown to regulate ischemia-induced angiogenesis [30]. MiR-126 augmented VEGF- and FGF-mediated angiogenic signaling by targeting Sprouty-related, EVH1 domain-containing protein 1 (Spred-1), an inhibitor of the Ras/MAP kinase pathway [31]. Moreover, endothelial miR-126 could regulate features of both angiogenesis and vasculogenesis. Those findings suggested a role for miR-126 in the maintenance of endothelial homeostasis [32–35]. Thus, we analyzed ischemic rabbit tissues for miR-126 expression to determine the effects of TFC and SIS on this important regulator of angiogenesis.

Material and Methods

Human and animal research approval

The collection of adipose tissue and blood from human volunteer was approved by the Ethics Committee of FN Ostrava (approval # 654/2014). All procedures involving animals were approved by the Local Ethics Committee of the Polish Academy of Science, Cracow, Poland (approval no. 1250/2015).

Indexed in: [Current Contents/Clinical Medicine] [SCI Expanded] [ISI Alerting System] [ISI Journals Master List] [Index Medicus/MEDLINE] [EMBASE/Excerpta Medica] [Chemical Abstracts/CAS]

Animals

A total of 30 female New Zealand White Rabbits (4–6 months old, 3.01±0.21 kg) were purchased from Zakład Doświadczalny Instytutu Zootechniki PIB, Chorzelów, Poland. The environmental controls on temperature and humidity were set according to the animal care standards of the Center for Cardiovascular Research and Development (Kostkowice, Poland). Animals were acclimated to the test facility at least 14 days prior to the start of the study. Sufficient food was provided for maintenance, and water was supplied ad libitum. Each rabbit had a unique ID number (Ear tag + tattoo). Body weights were recorded upon receipt and weekly thereafter, until the end of the study. The most recent body weight was used for calculation of all peri-operative medications. Body temperature was measured with a rectal probe thermometer.

Hindlimb ischemia surgery

On day 0, rabbits were anesthetized with an intramuscular (IM) injection of 20–40 mg/kg Ketamine (Bioketan 100 mg/ml, Vetoquinol, Gorzow Wielkopolski, Poland) and 5–10 mg/kg Xylazine (Xylapan 20 mg/ml, Vetoquinol, Gorzów Wielkopolski Poland); they also received a subcutaneous (SC) injection of 0.5 mg/kg Atropine (Atropinum Sulfuricum 1 mg/ml, Warszawskie Zakłady Farmaceutyczne Polfa, Warszawa, Poland). Additional intravascular (IV) boluses of 20–50 mg (0.2–0.5 ml) Ketamine were administered to maintain an appropriate depth of anesthesia during the surgical hind limb ischemia procedure. The femoral artery, its branches, and the femoral vein were ligated from the inguinal ligament to the bifurcation of the saphenous and popliteal arteries, and the intervening sections were excised. The incision was closed with stainless steel staples.

Post-surgical care

Rabbits were observed daily post-surgery for signs of infection, pain, and wound dehiscence. Cephalexin (20 mg/kg SC) was administered once per day (SID) (Cefalexim 18%, ScanVet, Warszawa, Poland) for 5 days as an antibiotic treatment. Carprofen (Arthropharm Pharmaceuticals, Inc., Ontario, Canada) was administered at 1.5 mg/kg, SC, SID for 3–4 days as an analgesic therapy. Additionally, animals were checked daily for any adverse events, until termination. At each follow-up time-point, anesthesia was performed with the same procedure outlined for day 0.

ASC isolation and TFC preparation

Adipose tissue was obtained from a 45-year-old female donor. The tissue was processed to isolate the SVF with a Cytori Celution device, as described previously [13]. Isolated SVF was processed to prepare TFC, as described previously [13].

Study groups and treatments

Rabbits with induced limb ischemia were randomly assigned to receive the following treatments: (1) Placebo control group: 5 ml Dulbecco's Modified Eagle's Medium (DMEM); (2) TFC group: 1 ml DMEM + 4 ml TFC; (3) SIS group: 4 ml. DMEM + 1 ml SIS; and (4) TFC + SIS group: 4 ml TFC + 1 ml SIS. Treatments were injected IM on day 7 after surgery with a 5-ml luer-lock syringe fitted with a 0.45×13 mm needle. Each dose of placebo, TFC, SIS, and TFC+SIS was divided into 5 parts: 2 parts were injected into each bundle (2 bundles) of the gastrocnemius muscle (4 injections), and one part was injected into the anterior tibial muscle. The injection volume was 1 ml per site.

Laser Doppler perfusion

Blood perfusion (expressed in relative perfusion units [RPU]) was measured in the skin and subcutaneous layers of the ischemic (left-INDEX) and intact (right-CONTROL) limbs with a Laser Doppler Perfilux 5000 device (Perimed, Järfälla, Sweden). Perfusion was measured on days 0 (before and after the surgery), 14, 28, 36, and 48.

Human ASC characterization with flow cytometry

The cells obtained in the SVF isolation procedure were resuspended and analyzed with flow cytometry to determine cell surface marker expression. Briefly, cells (2×10^5) were added to tubes containing complete medium (100 µl) and the tubes were maintained on ice. Fluorescently-conjugated monoclonal antibodies specific for cell surface markers, or isotype controls, were added (1 µl) to the tubes and incubated for 20-30 min on ice. Cells were subsequently washed with phosphate buffered saline (PBS), fixed in paraformaldehyde (Tousimis, Rockville, USA), and analyzed with a Cytomics FC500 (Beckman Coulter, Brea, CA, USA). The following antibody-conjugates (Beckman Coulter, Brea, CA, USA) were used: CD34-phycoerythrin (PE) (cat # A0776); CD34-Fluroscein isothiocyanate (FITC) (cat # IM1870); CD34-phycoerythrin/Cy5 (PC5) (cat # A07777); CD10-FITC (cat # IM0471U); CD29-PE (cat # 6604159); CD31 -PE (cat # IM2409); CD45-FITC (cat # A07782); CD45-ECD-R Phycoerythrin-Texas Red-X (cat # A07784); CD49-FITC (cat # IM1425); CD73-PE (cat # 344003); CD90-FITC (cat # IM1839U); CD105-PE (cat # A07414); CD13-PE/CD14-FITC (cat # A07722); and IgG1 isotype control-PE/FITC (cat # A07794).

Characterization of TFC

TFC samples were analyzed with ALBIA and ELISA to detect multiple human growth factors and cytokines. We employed Luminex screening assay kits (cat. no. LXSAHM-19, lot 1415713 and cat. no. LXSAHM-05, lot 1415707, from R&D Systems, Minneapolis, Minnesota, USA) for detecting the following

Indexed in: [Current Contents/Clinical Medicine] [SCI Expanded] [ISI Alerting System] [ISI Journals Master List] [Index Medicus/MEDLINE] [EMBASE/Excerpta Medica] [Chemical Abstracts/CAS]

factors: brain derived neurotrophic factor (BDNF), epithelial cell-derived neutrophil-activating peptide-78 (ENA-78), acidic fibroblast growth factor (aFGF), hepatocyte growth factor (HGF), interleukin-1β (IL-1β), interleukin-2 (IL-2), interleukin-4 (IL-4), interleukin-6 (IL-6), interleukin-7 (IL-7), interleukin-8 (IL-8), interleukin-10 (IL-10), interleukin-12 p70 (IL-12 p70), macrophage migration inhibitory factor (MIF), monocyte chemoattractant protein 1 (MCP1), matrix metalloproteinase-1 (MMP-1), matrix metalloproteinase-2 (MMP-2), matrix metalloproteinase-9 (MMP-9), stromal cell-derived factor 1 (SDF-1), tissue inhibitor of metalloproteinases 1 (TIMP-1), tumor necrosis factor α (TNFα), vascular endothelial growth factor (VEGF), interferon γ (IFN-γ), interleukin-13 (IL-13) and platelet-derived growth factor AA (PDGF-AA). We determined tumor necrosis factor-inducible gene 6 protein (TSG-6) expression with the ELISA kit, TNFAIP6/TSG-6-1β (LifeSpan BioSciences; Seattle, WA, USA). We performed insulin-like growth factor 2 (IGF-2) determinations with the Human IGF-2 ELISA kit (BioVendor – Laboratorní Medicína a.s., Brno, CZ). ALBIAs were measured with a Bio-Plex 200 (Bio – Rad laboratories, Inc., CA, USA) and analyzed with BioPlex Manager software, version 6.0 (Bio – Rad laboratories, Inc., CA, USA). Five-parameter logistic curves were applied for calibrations. ELISA measurements were performed with a Dynex MRX microplate reader (Dynex, Buštěhrad, CZ), and sample concentrations were evaluated with Myassays software (*http://www.myassays.com*). Four-parameter logistic curves were applied for calibrations.

Creation of micronized SIS

Sections of porcine jejunum were harvested from freshly-killed, mature, female pigs (culled sows) raised for human food production. Tissues were preserved under cryogenic conditions until further processing. Next, tissues were delaminated and decellularized with standardized, commercial processes, as described in US patents (#4,902,508 and 6,206,931) and in a published study. Short sections of hydrated SIS were then pinned to polymer boards, carefully lyophilized to a very low water content, milled in a Retsch tissue mill, and sieved to remove the largest particles. The final preparation contained a range of particle sizes, with a median size of 120 µm [36]. This micronized SIS preparation was packaged in gas-permeable bags and sterilized with ethylene oxide prior to shipment to the research facility.

Optimized binding of TFC to SIS

TFC binding to SIS was optimized prior to testing in the rabbit CLI model. A 2.5% (w/v) suspension of SIS (version 1.0 lyophilized powder, prototype, lot p118677, COOK Biotech Inc., Lafayette, IN, USA) was prepared by adding 0.1734 g of lyophilized SIS to 6.763 ml of PBS, and the suspension was stored at 4°C. This SIS suspension was added to a fixed volume (0.5 ml) of TFC to achieve final concentrations of 0.25, 0.5, 0.75, and 1% SIS. The total volume was adjusted to 1 ml with PBS. The suspensions were then mixed and incubated overnight at 37°C/5% CO_2. Next, the suspensions were centrifuged at 300×g for 10 min, and the liquid layers were removed to new tubes and stored at –70°C. The SIS was resuspended in 0.5 ml PBS, and the tubes were placed back in the incubator. After 24 h incubation the suspensions were centrifuged at 1500×g for 10 min, and the 0.1 ml of liquid layers were removed to new tubes and stored at –70°C. The rest of samples were resuspended and placed back in the incubator. This process was repeated once more for 96 h. Each collected supernatant was stored at -70°C until assayed with ELISA. The specific volumes and combinations tested were: (A) 0.5 ml TFC/0.5 ml PBS; (B) 0.1 ml SIS/0.5 ml TFC/0.4 ml PBS; (C) 0.2 ml SIS/0.5 ml TFC/0.3 ml PBS; (D) 0.3 ml SIS/0.5 ml TFC/0.2 ml PBS; (E) 0.4 ml SIS/0.5 ml CM/0.1 ml PBS; (F) 0.4 ml SIS/0.5 ml DMEM/0.1 ml PBS.

Histology

Immunohistochemistry

Formol-fixed tissue segments of gastrocnemius muscles were paraffin-embedded in blocks. The blocks were sectioned at a thickness of 2–4 µm, then stained with hematoxylin-eosin (H&E; Merck, Kenilworth, NJ). After examination of H&E-stained sections to confirm tissue integrity, additional sections were processed for immunohistochemical analyses. Detection of immunohistochemical markers (CD31 for endothelial cells and αSMA for smooth muscle cells) was performed with the Benchmark XT (Ventana Medical System). After blocking endogenous peroxidase activity and revitalizing the tissue antigens with CC1 buffer, the following primary antibodies were applied: monoclonal mouse anti-human CD31 (clone JCF0A, cat. No M0823, DakoCytomation, Glostrup, Denmark, dilution 1: 20) and monoclonal mouse anti-human αSMA (clone 1A4, cat. No M0851, DakoCytomation, Glostrup, Denmark, dilution 1: 100). Antigens were visualized with the staining system, iView DAB Detection Kit, and with hematoxylin counterstaining. Appendix tissue sections were used as positive and negative controls. We counted the numbers of positively stained vessels in a 10 mm^2 area of each block. Vessel density was calculated as the ratio of the ischemic (Index) limb value to the non-ischemic (Control) limb value.

In situ hybridization

From 29 rabbits, samples were acquired from paired gastrocnemius muscles, one from the normal and one from the ischemic hind limb of the same rabbit. The samples were embedded in paraffin blocks, and then cut into 2–4 µm sections. Sections were placed on Superfrost Plus® slides (Thermo Scientific, Waltham, MA, USA). The *in situ* hybridization (ISH) procedure

Indexed in: [Current Contents/Clinical Medicine] [SCI Expanded] [ISI Alerting System] [ISI Journals Master List] [Index Medicus/MEDLINE] [EMBASE/Excerpta Medica] [Chemical Abstracts/CAS]

was performed with the miRCURY LNA™ microRNA Detection (FFPE) kit (90005, Exiqon, Vedbaek, Denmark) according to the manufacturer's protocol. Briefly, proteinase K (0.5 µg/ml) was applied to tissue sections for 10 min at 37°C. The optimal probe concentration was previously established as 40 nM. After hybridization with the LNA probes in the kit, miR-126 molecules were visualized [37]. Stained sections were assessed under an Olympus BX40 (Olympus, Tokyo, Japan) optical microscope. The degree of miR-126 positivity in vessels and fibrous scars was scored on a semi-quantitative assessment scale, where 1=no or weak positivity and 2=moderate positivity. The positivity index was calculated separately for vessels and scars, and it was expressed as the number of samples with moderate miR-126 positivity out of the total number of samples in each treatment group.

Relative expression of miR-126 evaluated with quantitative RT-PCR

Total RNA was isolated from representative fresh frozen samples of the anterior tibial muscles and from healthy and ischemic rabbit hind limbs (N=29 rabbits) with the mirVana™ miRNA Isolation Kit (AM1560, Applied Biosystems, Foster City, CA, USA). Isolated RNA was reverse-transcribed with the TaqMan® MicroRNA Reverse Transcription Kit (4366596, Applied Biosystems, Foster City, CA, USA), which provided pooled gene-specific primers for detecting miR-126 (miR-126-3p) and RNU6B (RNA, U6 small nuclear 2) (Applied Biosystems, Foster City, CA, USA). The cDNA products were preamplified with the TaqMan® PreAmp Master Mix (2x) (4391128, Applied Biosystems, Foster City, CA, USA), and primers were provided in the pooled TaqMan® MicroRNA Assays (Applied Biosystems, Foster City, CA, USA) for detecting miR-126 and RNU6B. The miRNAs were evaluated with quantitative PCR (qPCR), performed with the TaqMan® Universal PCR Master Mix (2×) (4440047, Applied Biosystems, Foster City, CA, USA) and a miRNA specific probe from TaqMan® MicroRNA Assays (4427975, Assay ID: 002228 and 001093, Applied Biosystems, Foster City, CA, USA). RNU6B was used as an endogenous control. Real-time qPCR (RT-qPCR) was performed in triplicate on a LightCycler® 480 System (Roche, Branford, CT, USA). The entire procedure was performed according to the manufacturer's protocols. The relative expression of miR-126 was calculated with the $2^{-\Delta\Delta Ct}$ method [38]. We assume that, these relative expression levels were compared between the index and control limbs to obtain a miR-126 ratio (index/control limb). Finally, these ratios were compared between treatment groups.

Data representation and statistical analyses

Summary statistics are expressed as the arithmetic mean and standard deviation (mean ± sd). Most measurements are displayed as box and whisker plots (boxplots) to account for the strong non-Gaussian features of the data. On the boxplots, the central mark is the median; the top and bottom edges of the box are the 75th and 25th percentiles, respectively; the whiskers extend to the most extreme data points (not considering outliers), which are marked with the black dots. Also, the ordinal scatter plots are used for better representation of data which could possibly distinguish individual animals in the sense of extreme values within particular group. To test the key statistical hypotheses about the treatment groups, all the endpoints were compared between groups with Kruskal Wallis, Mann Whitney, or Welch t-tests, according to their suitability for the particular statistical properties (probability density moments) of the distributions of the measurements. In addition to classical statistics, an alternative approach of gnostics was used to analyze and validate our findings [39,40].

Results

Characterization of TFC

Freshly isolated SVF and cultured cells displayed the cell surface markers typical of human adipose tissue-derived populations (Table 1). After cells were cultured for 4 passages, the population possessed surface marker profiles typical of ASC; they were uniformly positive for the mesenchymal surface markers, CD13 and CD73, and did not co-express endothelial (CD31) or hematopoietic (CD45) surface markers. The levels of selected growth factors and cytokines in the TFC derived from the passaged cells, are given in Table 2. The profile of measured factors was very similar to that obtained in a previous study, with the exception that we found higher levels of IL-2, IL-4, and IL-8 [13]. This TFC was used for treating rabbits with CLI.

Optimization of the TFC and SIS combination

The optimal binding and release kinetics were determined by incubating a set concentration of TFC with various amounts of SIS, and then following the release of selected factors, when resuspended in PBS (Figure 1). The input concentrations of aFGF, VEGF, and HGF (first column) were compared to the unbound concentrations following incubation with SIS (columns 2, 5, 8, and 11). We found that the lowest concentration of SIS (0.25%) induced near maximal binding capacity for these 3 factors. Furthermore, the apparent release kinetics of the measured factors were slower at this SIS concentration than at the higher concentrations (0.5–1.5%). Based on these data, we used a ratio of 1 ml TFC to 0.5% SIS for the *in vivo* studies.

Reperfusion of hindlimb ischemia

A total of 30 animals were included in the study. One rabbit in the SIS treatment group died on day 36, but all other animals completed the entire study. The weights and temperatures of

Indexed in: [Current Contents/Clinical Medicine] [SCI Expanded] [ISI Alerting System] [ISI Journals Master List] [Index Medicus/MEDLINE] [EMBASE/Excerpta Medica] [Chemical Abstracts/CAS]

Table 1. Characterization and distribution of cell populations in freshly obtained SVF and cultured ASCs derived from human adipose tissue.

Suspension	Fresh SVF		P1 ASCs	P4 ASCs
CD markers	[a]CD34+		[b]CD34–	
CD45–	37.0	25.7	99.2	99.36
CD45+	6.6	30.9	<1	<1
CD105+	<1	<1	76.9	52.6
CD13+	84.5	11.2	99.7	99.9
CD10+	<1	<1	38.0	13.1
CD31+	5.9	5.5	19.6	<1
CD90+	80.5	13.5	38.4	1.1
CD14+	<1	<1	<1	<1
CD29+	80.0	<1	95.8	98.6
CD49+	<1	<1	1.7	<1
CD73+	80.4	<1	98.7	99.8

Values are the percentage of cell populations in freshly prepared non-adipocyte stromal vascular fraction (SVF) and cultured adipose tissue-derived stem cells (ASCs) in passage 1 (P1) and passage 4 (P4). Cell markers were evaluated with flow cytometry. [a] Fresh SVF contained 44% CD34+ cells; [b] P1 and P4 passages contained <1% CD34+ cells.

Table 2. Concentrations of selected proteins in human TFC used to treat ischemia in a rabbit model of CLI.

Protein	pg/ml	Protein	pg/ml
IFN-γ	33	BDNF	41
IGF II	133,000	aFGF	203
IL-1β	16	HGF	15,966
IL-2	1,103	PDGF-AA	48
IL-4	435	SDF-1α	941
IL-6	952	TIMP-1	>850,000
IL-7	73	TSG-6	11,000
IL-8/CXCL8	1,991	VEGF	11,360
IL-10	4	MMP-1	11,090
IL-12 p70	636	MMP-2	717,351
IL13	989	MMP-9	55
MCP-1/CCL2	9,324	ENA-78/CXCL5	3,736
TNF-α	8	MIF	315,801

the animals remained within normal levels with no differences between groups during the study period (Figure 2). We measured blood perfusion in the left (index) ischemic and right (control) intact limbs. Measurements were performed in the lower hindlimb, as described previously [13] (Figure 3). On day 28, the index/control perfusion was significantly higher in the TFC, SIS, and TFC+SIS groups, compared to placebo (p=0.0816, p=0.05428, and p=0.0639, respectively). Enhanced index/control perfusion (compared to placebo) was maintained on day 36 in the TFC group (p=0.0866), but not in the other groups. Perfusion was not significantly different among groups by day 48 (Figure 4).

Vessel density

Vessel density was calculated as the ratio of the ischemic (Index) limb value to the non-ischemic (Control) limb value. We

Indexed in: [Current Contents/Clinical Medicine] [SCI Expanded] [ISI Alerting System] [ISI Journals Master List] [Index Medicus/MEDLINE] [EMBASE/Excerpta Medica] [Chemical Abstracts/CAS]

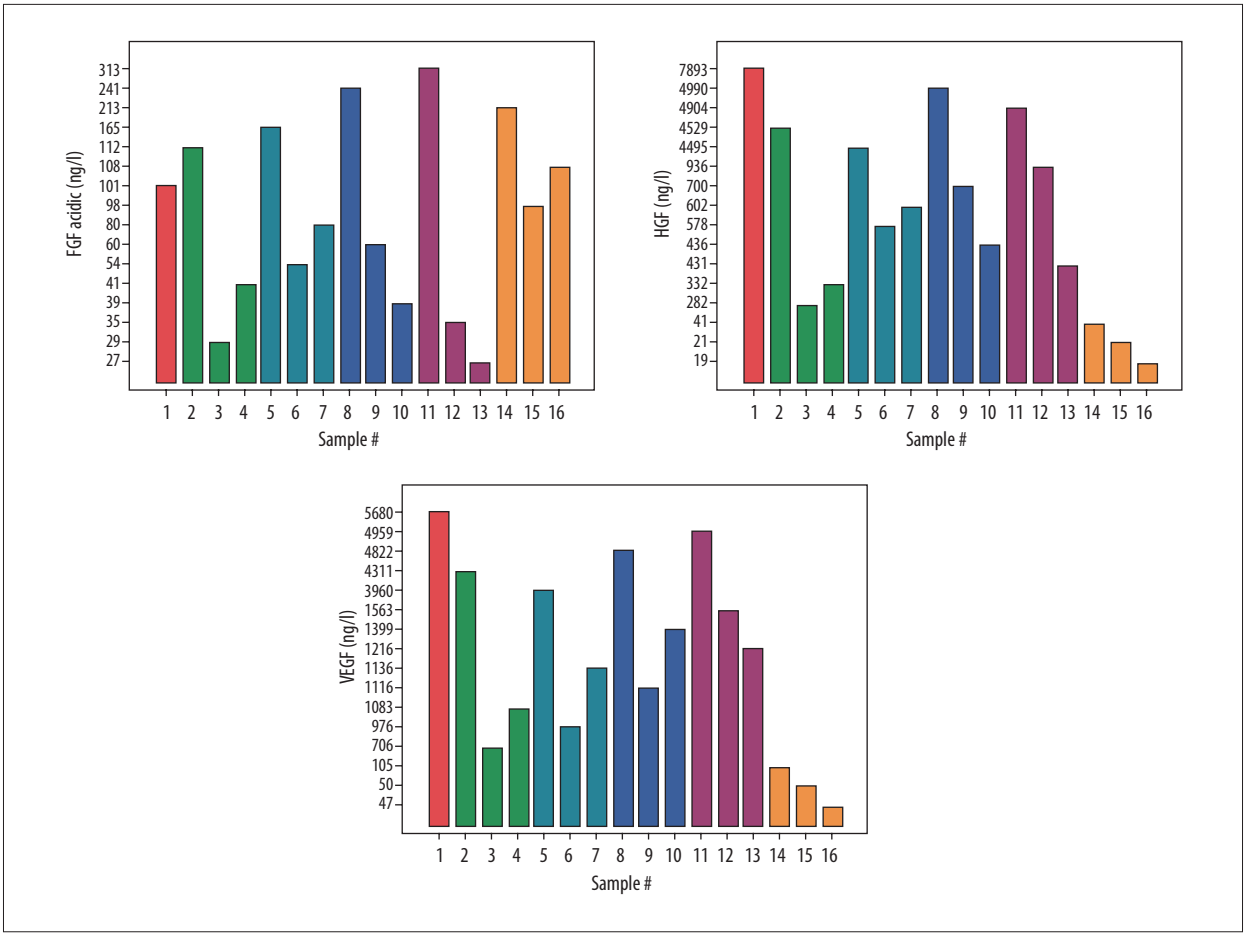

Figure 1. Optimizing TFC binding to SIS and determining kinetics of growth factor release. The levels of aFGF, HGF, and VEGF in twice-diluted TFC (red bar 1). TFC (0.5 ml) was incubated overnight with different ratios of SIS: PBS to promote binding. The unbound levels of aFGF, HGF, and VEGF after incubation were quantified in the supernatants of these cultures (bars 2, 5, 8, 11, and 14). Pellets of these cultures were re-suspended in DMEM and incubated at 37°C for 24 h (bars 3, 6, 9, 12, and 15) and 96 h (bars 4, 7, 10, 13, and 16). Supernatants were collected, and the levels of the indicated growth factors were determined. The mixtures contained TFC (0.5 ml, constant), and the following combinations of SIS to PBS: 0.1 ml SIS + 0.4 ml PBS (green bars 2–4), 0.2 ml SIS + 0.3 ml PBS (pale blue bars 5–7), 0.3 ml SIS + 0.2 ml PBS (blue bars 8–10), 0.4 ml SIS + 0.1 ml PBS (violet bars 11–13), and 0.5 ml SIS (orange bars 14–16). The total volume for each sample was 1 ml.

counted all vessels positively stained for CD31 and αSMA antigens (Figure 5). The index/control ratios of $CD31^+$ capillary densities were significantly higher in the SIS and TFC+SIS groups compared to the placebo group (p=0.0093 and 0.0054, respectively) (Figure 5A). The index/control ratios of αSMA-stained vessel densities (presumably small arterioles) was higher in the SIS group (p=0.0305) than in the placebo group (Figure 5B).

Quantitative analysis of miR-126 expression

We evaluated the expression of an important regulator of angiogenesis, miR-126, in gastrocnemius muscle samples. The qRT-PCR results were evaluated with the $2^{-\Delta\Delta Ct}$ method. The target gene expression levels in the index limb were compared to levels in the control limb of each animal. The absolute levels of miR-126 were very low in the tissues measured in the placebo, TFC, SIS and TFC+SIS groups. The low levels of miR-126 detected with qRT-PCR may reflect the restricted expression of this RNA species to endothelial cells and well-vascularized tissues [41]. The ratios (index/control limb) of miR-126 expression were: 1.35±1.4 (control); 1.32±1.81 (TFC); 2.3±1.91 (SIS); and 2.9±3.07 (TFC+SIS). We observed a trend of higher miR-126 expression in the SIS and TFC+SIS groups (p=0.1161 and 0.1967 respectively) compared to the placebo and TFC groups (Figure 6). Although these values were not significantly different, they did correlate with vessel density measurements. This observation suggested that angiogenesis was actively promoted by miR-126 on day 48 after the induction of ischemia (Figure 5).

Indexed in: [Current Contents/Clinical Medicine] [SCI Expanded] [ISI Alerting System] [ISI Journals Master List] [Index Medicus/MEDLINE] [EMBASE/Excerpta Medica] [Chemical Abstracts/CAS]

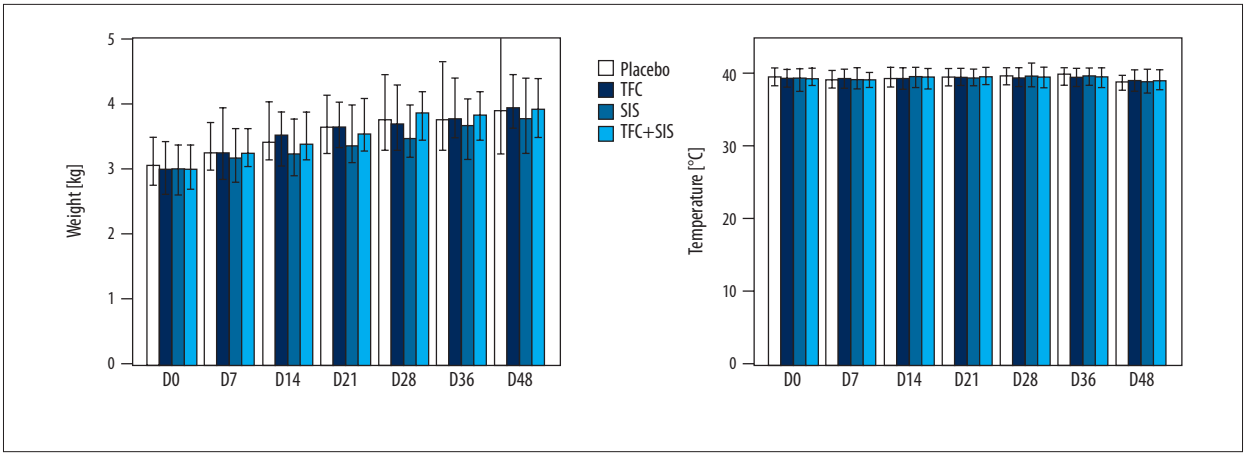

Figure 2. Weight and temperature analysis of rabbits during treatment. Day 0 to day 48 measurements of weight and temperature; the medians and robust lower and upper bounds are plotted. No adverse elevation in body temperature and no significant differences in normal weight were observed after TFC, SIS, or TFC+SIS were administered in the rabbit groups during the period of observation.

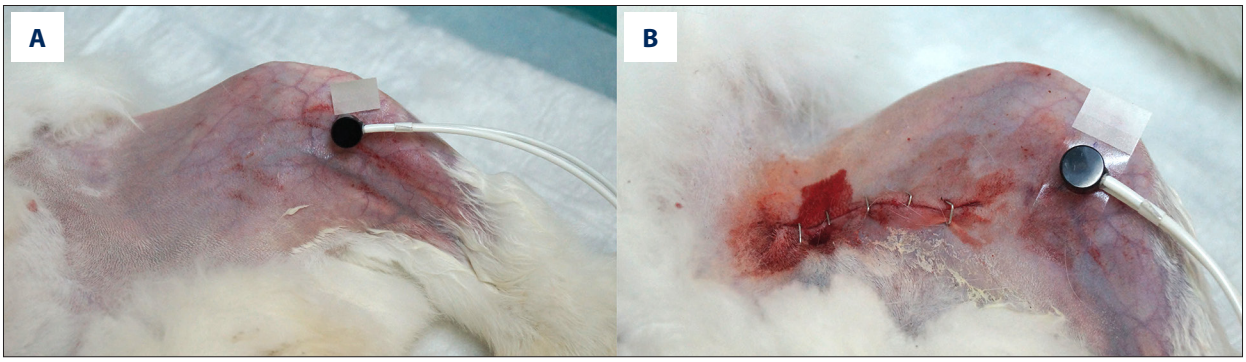

Figure 3. Skin perfusion analysis. Skin perfusion was measured with a Periflux 5000 contact probe. Laser Doppler flow was measured at the level of the gastrocnemius muscle (**A**) before surgery; (**B**) after SFA ligation and extraction, perfusion was measured at the same position.

Histomorphology and *in situ* hybridization of miR-126

All tissues from each group that were evaluated with H&E exhibited characteristics of the late stages of healing, such as active maturation of fibrous scars (Figure 7). We performed ISH to detect miR-126 in gastrocnemius muscle tissues to determine whether its expression correlated with structural evidence of tissue repair and reperfusion. Positive staining for miR-126 was observed in the vascular endothelium, the smooth muscle cells of the arterioles, the cellular elements of fibrous scars, and in the sarcoplasm of some muscle fibers. Overall, miR-126 positivity was relatively low in tissues on day 48. More distinctive miR-126 positivity in blood vessels (indicating ongoing angiogenesis) was observed in the samples from the SIS and TFC+SIS groups compared to samples from the placebo group. Tissue samples from limbs treated with TFC alone were virtually miR-126-negative.

The degree of miR-126 positivity in vessels and fibrous scars was assessed semi-quantitatively, based on a tissue scoring system. Samples were scored as: 1=no or weak positivity, or 2=moderate positivity. The positivity index was calculated separately for vessels and scars, and it was expressed as the number of samples with moderate miR-126 positivity out of the total number of samples in each treatment group. The miR-126 positivity indexes in vessels were: placebo, 0.33; TFC, 0; SIS, 0.29; and TFC+SIS, 0.13. The indexes for scar regions were: placebo 0.33; TFC, 0; SIS, 0.13; and TFC+SIS, 0.25.

Discussion

Treating ischemic tissues with ASC-derived TFC is a potential alternative therapy to stem cell injections [42–44]. Our previous study demonstrated robust dose-dependent repair with a single IM bolus of TFC in a rabbit model of CLI [13]. In the present study, we tested the potential for enhancing this effect

Indexed in: [Current Contents/Clinical Medicine] [SCI Expanded] [ISI Alerting System] [ISI Journals Master List] [Index Medicus/MEDLINE] [EMBASE/Excerpta Medica] [Chemical Abstracts/CAS]

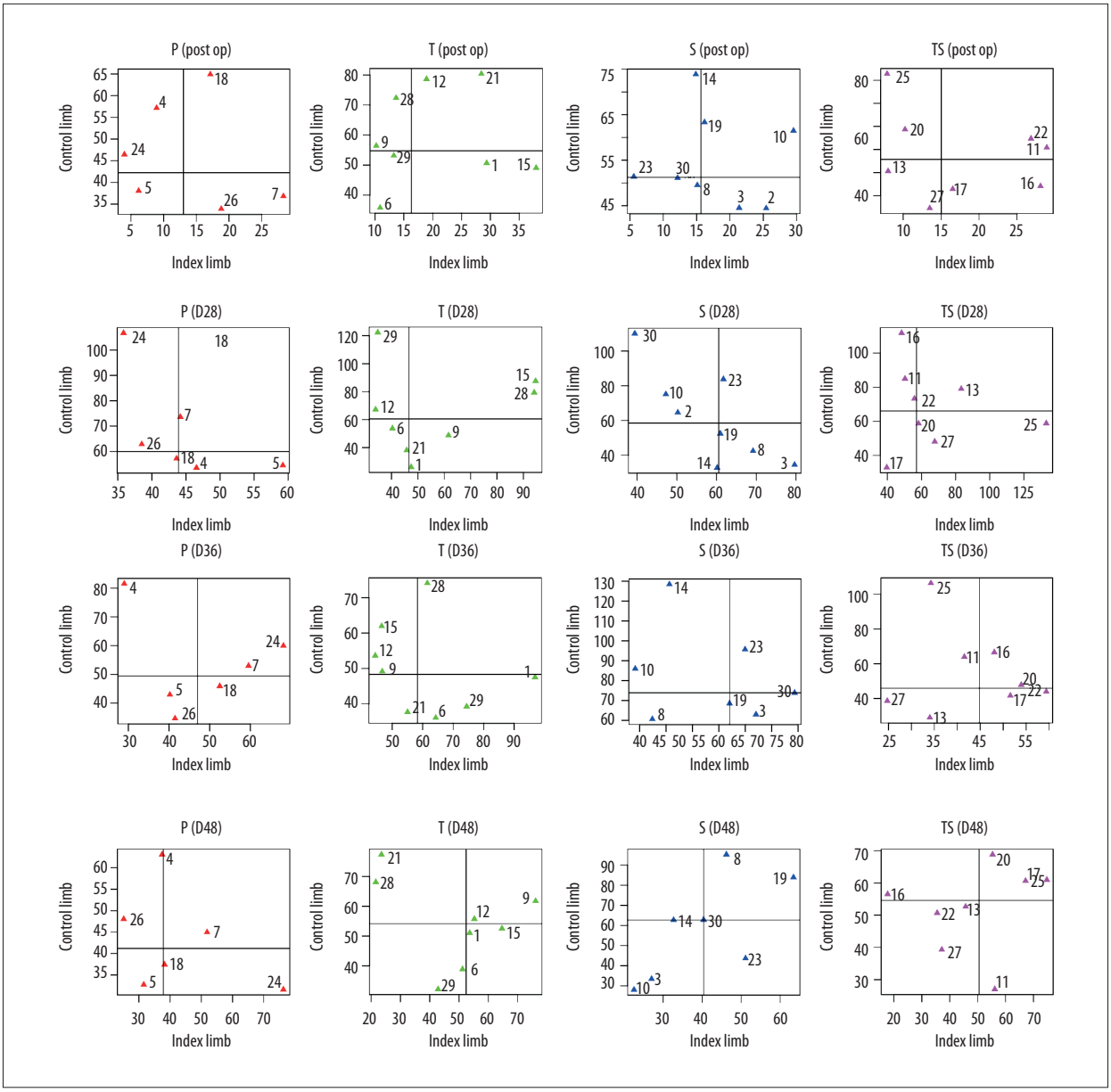

Figure 4. Laser Doppler skin perfusion. Ordinal scatter plots for days 0 to 48 with marked individual animals, showing the development of the index/control perfusion ratio in individual animals. We also compared dispersion of data within graphs which contain values measured at the same time. Changes within particular group in the observed time can also be seen. LDP is expressed as the ratio of relative perfusion units (RPU) in the index limb/control limb. Measurements are shown for days 0 to 48**.** The index/control perfusion ratios on day 28 in the TFC, SIS, and TFC+SIS groups were significantly higher than that in the placebo control group (p=0.0816, p=0.0543, and p=0.0639, respectively). The index/control perfusion ratio on day 36 was significantly higher in the TFC group (p=0.0866) than in the placebo group, (P=placebo, T=TFC, S=SIS, TS=TFC+SIS).

by combining TFC with the biological matrix, micronized SIS. We reasoned that, as a carrier, SIS possessed properties that could be additive to TFC action. SIS possesses a microstructure that is conducive to the attachment and growth of immigrating reparative cells and its composition facilitates the binding and release of associated growth factors. Independent of TFC, growth factors have the potential to stimulate endogenous repair, modulate inflammation, and promote survival of at-risk tissues [20]. Additionally, the factors that are inherently associated with SIS could complement the factors associated with TFC. For instance, we measured much higher concentrations of FGF-2 in SIS than in TFC. Thus, SIS could serve as a biological "sponge" for TFC components, a scaffold for reparative cells migrating into the injury site, and a sink for therapeutic factors [45].

Indexed in: [Current Contents/Clinical Medicine] [SCI Expanded] [ISI Alerting System] [ISI Journals Master List] [Index Medicus/MEDLINE] [EMBASE/Excerpta Medica] [Chemical Abstracts/CAS]

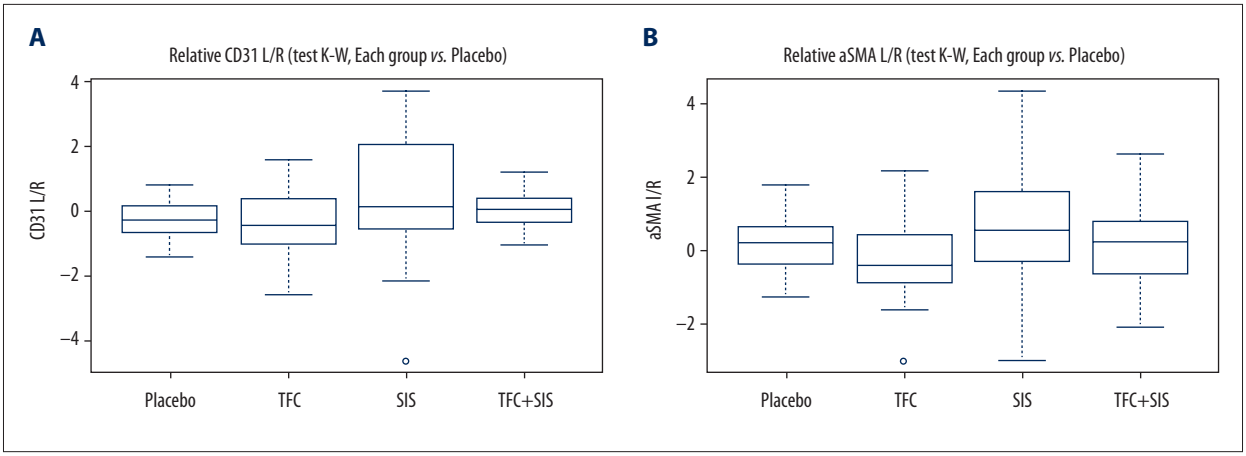

Figure 5. Vessel density measurement. (**A**) Ratios of CD31+ capillary densities (ischemic/control limb) measured in the gastrocnemius muscles. Ischemic/control ratios in the SIS and TFC+SIS groups were significantly higher than in the controls (p=0.0093 and p=0.0054, respectively). (**B**) Ratios of αSMA+ vessel densities in ischemic/control limbs. No difference between groups was observed.

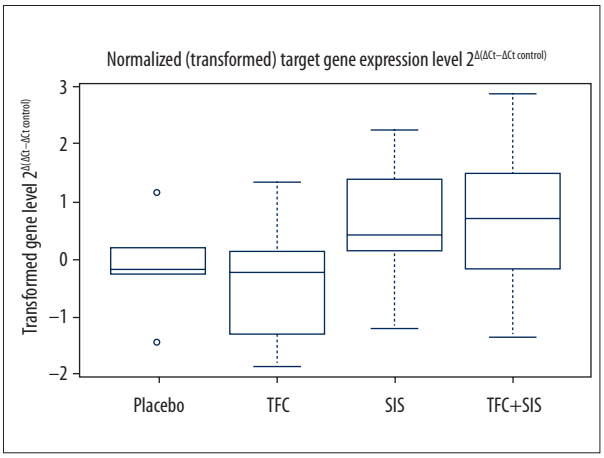

Figure 6. Target gene expression. The ratios of the index limb/control limb showed trends (p>0.05) of higher miR-126 expression in the SIS (p=0.1161) and SIS+TFC (p=0.1967) groups, compared to the placebo group; these results are consistent with results found with the index limb perfusion measurements performed with the laser Doppler technique. Relative gene expression levels were calculated with the $2^{-\Delta\Delta Ct}$ method. Target gene expression in the index limb was compared to expression in the control limb from all distribution groups, and transformed with a Box-Cox power transformation.

In the present study, although LDP showed that TFC significantly enhanced tissue perfusion, the effect was somewhat attenuated, compared to the effect observed previously [13]. A partial explanation for this discrepancy might be that these 2 studies differed with respect to the donor adipose from which the ASC samples were isolated. In fact, the cells used in the present study secreted higher levels of IL-2, IL-4, and IL-8 compared to cells in the previous study. Interleukins are classically defined as T-cell stimulators, and they have recently been shown to have dual functions, depending on the concentration. For instance, IL-8 is proangiogenic at low concentrations and proinflammatory at high concentrations [46]. Thus, higher levels of these factors in the TFC used in the present study may have negatively contributed to TFC potency.

The effects of TFC and SIS on repair of ischemic hind limb muscles were equivalent; we observed no additive effect with the combination. However, the reparative process appeared to be prolonged with SIS treatment compared to TFC treatment. This was evidenced by the increased microvessel density observed at 48 days with SIS treatment (either alone or in combination with TFC). Interestingly, miR126 levels in ischemic tissues in the TFC group were lower than miR-126 levels in the placebo and SIS groups. This regulatory RNA species is a master regulator of adult neoangiogenesis in response to ischemic injury. Antagonism of miR-126 severely attenuated recovery of tissue perfusion in a mouse model of hind limb ischemia [33]. This effect of TFC on miR-126 was not observed when TFC was combined with SIS. A potential explanation for this observation might be that TFC promoted rapid healing, but in the later period (48 days after ischemia), when miR-126 was analyzed, the TFC effects may have been completed. In contrast, SIS had sustained effects, due to its longer-term physical presence in tissues; thus, it continued to promote some repair.

Another interesting finding from this study was the ISH detection of miR-126 in muscle tissues. Previously, miR-126 was reported to be an endothelial-restricted miRNA. However, we detected miR-126 in other cellular elements, including in the smooth muscle cells of arterioles, in fibrous scars, and in the sarcoplasm of some muscle fibers. These data suggested that miR-126 had a broader tissue distribution than previously reported, at least under pathological conditions [47].

Indexed in: [Current Contents/Clinical Medicine] [SCI Expanded] [ISI Alerting System] [ISI Journals Master List] [Index Medicus/MEDLINE] [EMBASE/Excerpta Medica] [Chemical Abstracts/CAS]

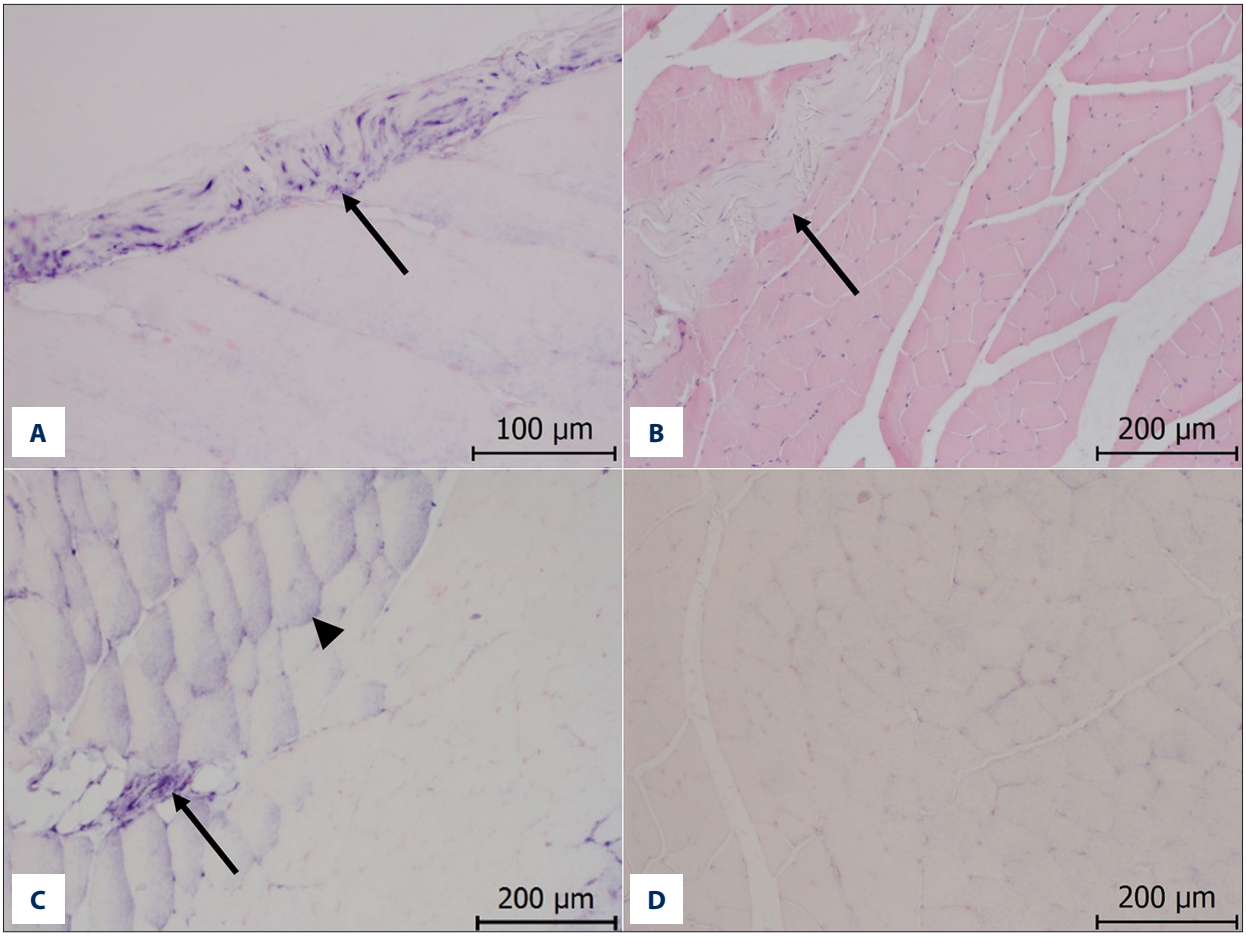

Figure 7. Detection of miR-126 molecules with *in situ* hybridization. Muscle tissue sections were probed with *in situ* hybridization to evaluate miR-126 expression and stained with H&E to visualize cellular structures. MiR-126 positivity was demonstrated in the following tissue structures: vascular endothelium, smooth muscle cells of the arterioles, cellular elements of fibrous scars, and in the sarcoplasm of some muscle fibers. (**A**) miR-126 positivity (blue) in the cell elements of a maturating scar (arrow); (**B**) the fibrous scar (arrow) in H&E staining; (**C**) miR-126 positivity (blue) in the vessels (arrow) and sarcoplasm of muscle fibers (arrowhead); (**D**) miR-126 negative tissue.

Conclusions

A rabbit limb ischemia model was constructed to confirm the hypothesis that miR-126 has role in CLI treatment using Adipose-Derived Stem Cell Therapeutic Factor Concentrate and Extracellular Matrix Microparticles. The influence of miR-126 on angiogenesis and vasculogenesis regulation has been tested using a quantitative analysis of miR-126 expression, histomorphology, and *in situ* hybridization of ischemic rabbit tissues.

For better understanding of the role of miR-126 in angiogenesis and vasculogenesis, it will be suitable to monitor changes of analyzed parameters in different phases of reparative process in time. These preliminary results showed that expression level of miR-126 reflects successful reparation of ischemic hind limb muscles after the treatment application, but it should be confirmed by studies with larger sample groups.

These results support our hypothesis that TFC can be used as an alternative to cellular therapy for the treatment of critical limb ischemia. We reasoned that it might be possible to enhance the effect of TFC by combining it with a carrier, as tested in this study, and to promote sustained release of repair factors in the target tissue. Future studies will be directed towards optimizing this combination. A successful treatment might increase the quality of life and reduce morbidities (such as amputations) for a significant population of patients with CLI that currently lacks sufficient improvement with conventional therapy.

Conflict of interest

None.

Indexed in: [Current Contents/Clinical Medicine] [SCI Expanded] [ISI Alerting System] [ISI Journals Master List] [Index Medicus/MEDLINE] [EMBASE/Excerpta Medica] [Chemical Abstracts/CAS]

References:

1. Traktuev DO, Merfeld-Clauss S, Li J et al: A population of multipotent CD34-positive adipose stromal cells share pericyte and mesenchymal surface markers, reside in a periendothelial location, and stabilize endothelial networks. Circ Res, 2008; 102(1): 77–85
2. Bourin P, Bunnell BA, Casteilla L et al: Stromal cells from the adipose tissue-derived stromal vascular fraction and culture expanded adipose tissue-derived stromal/stem cells: A joint statement of the International Federation for Adipose Therapeutics and Science (IFATS) and the International Society for Cellular Therapy (ISCT). Cytotherapy, 2013; 15(6): 641–48
3. Miranville A, Heeschen C, Sengenes C et al: Improvement of postnatal neovascularization by human adipose tissue-derived stem cells. Circulation, 2004; 110(3): 349–55
4. Moon MH, Kim SY, Kim YJ et al: Human adipose tissue-derived mesenchymal stem cells improve postnatal neovascularization in a mouse model of hindlimb ischemia. Cell Physiol Biochem, 2006; 17(5–6): 279–90
5. Nakagami H, Maeda K, Morishita R et al: Novel autologous cell therapy in ischemic limb disease through growth factor secretion by cultured adipose tissue-derived stromal cells. Arterioscler Thromb Vasc Biol, 2005; 25(12): 2542–47
6. Planat-Benard V, Silvestre JS, Cousin B et al: Plasticity of human adipose lineage cells toward endothelial cells: Physiological and therapeutic perspectives. Circulation, 2004; 109(5): 656–63
7. Rehman J, Traktuev D, Li J et al: Secretion of angiogenic and antiapoptotic factors by human adipose stromal cells. Circulation, 2004; 109(10): 1292–98
8. Bura A, Planat-Benard V, Bourin P et al: Phase I trial: the use of autologous cultured adipose-derived stroma/stem cells to treat patients with non-revascularizable critical limb ischemia. Cytotherapy, 2014; 16(2): 245–57
9. Caplan AI, Dennis JE: Mesenchymal stem cells as trophic mediators. J Cell Biochem, 2006; 98(5): 1076–84
10. Kinnaird T, Stabile E, Burnett MS et al: Marrow-derived stromal cells express genes encoding a broad spectrum of arteriogenic cytokines and promote *in vitro* and *in vivo* arteriogenesis through paracrine mechanisms. Circ Res, 2004; 94(5): 678–85
11. Murphy MB, Moncivais K, Caplan AI: Mesenchymal stem cells: Environmentally responsive therapeutics for regenerative medicine. Exp Mol Med, 2013; 45: e54
12. Gnecchi M, Zhang Z, Ni A, Dzau VJ: Paracrine mechanisms in adult stem cell signaling and therapy. Circ Res, 2008; 103(11): 1204–19
13. Prochazka V, Jurcikova J, Lassak O et al: Therapeutic potential of adipose-derived therapeutic factor concentrate for treating critical limb ischemia. Cell Transplant, 2016; 25(9): 1623–33
14. Bissell MJ, Aggeler J: Dynamic reciprocity: How do extracellular matrix and hormones direct gene expression? Prog Clin Biol Res, 1987; 249: 251–62
15. Ori A, Wilkinson MC, Fernig DG: The heparanome and regulation of cell function: Structures, functions and challenges. Front Biosci, 2008; 13: 4309–38
16. Lau EK, Paavola CD, Johnson Z et al: Identification of the glycosaminoglycan binding site of the CC chemokine, MCP-1: Implications for structure and function *in vivo*. J Biol Chem, 2004; 279(21): 22294–305
17. Sepuru KM, Nagarajan B, Desai UR, Rajarathnam K: Molecular Basis of Chemokine CXCL5-Glycosaminoglycan Interactions. J Biol Chem, 2016; 291(39): 20539–50
18. Hodde J, Janis A, Ernst D et al: Effects of sterilization on an extracellular matrix scaffold: Part I. Composition and matrix architecture. J Mater Sci Mater Med, 2007; 18(4): 537–43
19. Qiang B, Lim SY, Lekas M et al: Perlecan heparan sulfate proteoglycan is a critical determinant of angiogenesis in response to mouse hind-limb ischemia. Can J Cardiol, 2014; 30(11): 1444–51
20. Chang J, DeLillo N Jr., Khan M, Nacinovich MR: Review of small intestine submucosa extracellular matrix technology in multiple difficult-to-treat wound types. Wounds, 2013; 25(5): 113–20
21. O'Donnell TF Jr., Lau J: A systematic review of randomized controlled trials of wound dressings for chronic venous ulcer. J Vasc Surg, 2006; 44(5): 1118–25
22. Hiles M, Hodde J: Tissue engineering a clinically useful extracellular matrix biomaterial. Int Urogynecol J Pelvic Floor Dysfunct, 2006; 17(Suppl. 1): S39–43
23. Hodde J: Naturally occurring scaffolds for soft tissue repair and regeneration. Tissue Eng, 2002; 8(2): 295–308
24. Hodde J: Extracellular matrix as a bioactive material for soft tissue reconstruction. ANZ J Surg, 2006; 76(12): 1096–100
25. Hodde J, Hiles M: Constructive soft tissue remodelling with a biologic extracellular matrix graft: Overview and review of the clinical literature. Acta Chir Belg, 2007; 107(6): 641–47
26. Hodde JP, Record RD, Liang HA, Badylak SF: Vascular endothelial growth factor in porcine-derived extracellular matrix. Endothelium, 2001; 8(1): 11–24
27. Lee RC, Feinbaum RL, Ambros V: The C. elegans heterochronic gene lin-4 encodes small RNAs with antisense complementarity to lin-14. Cell, 1993; 75(5): 843–54
28. Filipowicz W, Bhattacharyya SN, Sonenberg N: Mechanisms of post-transcriptional regulation by microRNAs: Are the answers in sight? Nat Rev Genet, 2008; 9(2): 102–14
29. Fish JE: A primer on the role of microRNAs in endothelial biology and vascular disease. Semin Nephrol, 2012; 32(2): 167–75
30. Caporali A, Emanueli C: MicroRNA regulation in angiogenesis. Vascul Pharmacol, 2011; 55(4): 79–86
31. Wang S, Aurora AB, Johnson BA et al: The endothelial-specific microRNA miR-126 governs vascular integrity and angiogenesis. Dev Cell, 2008; 15(2): 261–71
32. Wu F, Yang Z, Li G: Role of specific microRNAs for endothelial function and angiogenesis. Biochem Biophys Res Commun, 2009; 386(4): 549–53
33. van Solingen C, Seghers L, Bijkerk R et al: Antagomir-mediated silencing of endothelial cell specific microRNA-126 impairs ischemia-induced angiogenesis. J Cell Mol Med, 2009; 13(8A): 1577–85
34. van Solingen C, de Boer HC, Bijkerk R et al: MicroRNA-126 modulates endothelial SDF-1 expression and mobilization of Sca-1(+)/Lin (–) progenitor cells in ischaemia. Cardiovasc Res, 2011; 92(3): 449–55
35. Kartha RV, Subramanian S: MicroRNAs in cardiovascular diseases: Biology and potential clinical applications. J Cardiovasc Transl Res, 2010; 3(3): 256–70
36. Badylak SF, Lantz GC, Coffey A, Geddes LA: Small intestinal submucosa as a large diameter vascular graft in the dog. J Surg Res, 1989; 47(1): 74–80
37. Jorgensen S, Baker A, Moller S, Nielsen BS: Robust one-day *in situ* hybridization protocol for detection of microRNAs in paraffin samples using LNA probes. Methods, 2010; 52(4): 375–81
38. Livak KJ, Schmittgen TD: Analysis of relative gene expression data using real-time quantitative PCR and the 2(-Delta Delta C(T)) method. Methods, 2001; 25(4): 402–8
39. Kovanic P, Huber MB: The Economics of Information – Mathematical Gnostics for Data Analysis: 2003; *www.math-gnostics.com*
40. Kovanic POT, Grabic R, Rieder M: Gnostic Analysis: A novel approach for univariate and multivariate data analysis. applications to experimental data from monitoring and research. In: Nagib C R-HC, Sylvain F, Rabin Raut ZH (eds.), 9th World Multi-Conference on Systemics, Cybernetics and Informatics WMSCI 2005;. Orlando, Florida, USA: IIIS Copyright Manager, 14269 Lord Barclay Dr., Orlando, Fl. 32837, USA, 2005; 289–64
41. Landgraf P, Rusu M, Sheridan R et al: A mammalian microRNA expression atlas based on small RNA library sequencing. Cell, 2007; 129(7): 1401–14
42. Amann B, Luedemann C, Ratei R et al: Autologous bone marrow cell transplantation increases leg perfusion and reduces amputations in patients with advanced critical limb ischemia due to peripheral artery disease. Cell Transplant, 2009; 18(3): 371–80
43. Benoit E, O'Donnell TF, Patel AN: Safety and efficacy of autologous cell therapy in critical limb ischemia: A systematic review. Cell Transplant, 2013; 22(3): 545–62
44. Procházka V, Gumulec J, Jalůvka F et al: Cell therapy, a new standard in management of chronic critical limb ischemia and foot ulcer. Cell Transplant, 2010; 19(11): 1413–24
45. Mostow EN, Haraway GD, Dalsing M et al. OASIS Venus Ulcer Study Group: Effectiveness of an extracellular matrix graft (OASIS Wound Matrix) in the treatment of chronic leg ulcers: a randomized clinical trial. J Vasc Surg, 2005; 41(5): 837–43
46. Strieter RM, Kunkel SL, Elner VM et al: Interleukin-8. A corneal factor that induces neovascularization. Am J Pathol, 1992; 141(6): 1279–84
47. Boon RA, Dimmeler S: MicroRNA-126 in atherosclerosis. Arterioscler Thromb Vasc Biol, 2014; 34(7): e15–16

Indexed in: [Current Contents/Clinical Medicine] [SCI Expanded] [ISI Alerting System] [ISI Journals Master List] [Index Medicus/MEDLINE] [EMBASE/Excerpta Medica] [Chemical Abstracts/CAS]